Photosynthesis Research (2024) 159:61–68
https://doi.org/10.1007/s11120-023-01073-3

RESEARCH

Extra O_2 evolution reveals an O_2-independent alternative electron sink in photosynthesis of marine diatoms

Ginga Shimakawa[1] · **Yusuke Matsuda**[1]

Received: 31 August 2023 / Accepted: 27 December 2023 / Published online: 5 February 2024

Abstract

Following the principle of oxygenic photosynthesis, electron transport in the thylakoid membranes (i.e., light reaction) generates ATP and NADPH from light energy, which is subsequently utilized for CO_2 fixation in the Calvin-Benson-Bassham cycle (i.e., dark reaction). However, light and dark reactions could discord when an alternative electron flow occurs with a rate comparable to the linear electron flow. Here, we quantitatively monitored O_2 and total dissolved inorganic carbon (DIC) during photosynthesis in the pennate diatom *Phaeodactylum tricornutum*, and found that evolved O_2 was larger than the consumption of DIC, which was consistent with $^{14}CO_2$ measurements in literature. In our measurements, the stoichiometry of O_2 evolution to DIC consumption was always around 1.5 during photosynthesis at different DIC concentrations. The same stoichiometry was observed in the cells grown under different CO_2 concentrations and nitrogen sources except for the nitrogen-starved cells showing O_2 evolution 2.5 times larger than DIC consumption. An inhibitor to nitrogen assimilation did not affect the extra O_2 evolution. Further, the same physiological phenomenon was observed in the centric diatom *Thalassiosira pseudonana*. Based on the present dataset, we propose that the marine diatoms possess the metabolic pathway(s) functioning as the O_2-independent electron sink under steady state photosynthesis that reaches nearly half of electron flux of the Calvin-Benson-Bassham cycle.

Keywords Photosynthesis · Oxygen · Dissolved inorganic carbon · Marine diatoms

Introduction

Oxygenic photosynthesis is the most important biological reaction for primary production on earth, and occurs at almost equal amount on land and under water (Field et al. 1998). The fundamental principle of oxygenic photosynthesis had been uncovered mainly in the isolated chloroplasts and intact leaves of plants, giving the common knowledge of the coupling of light and dark reactions of photosynthesis (Bishop 1971; Farquhar et al. 1980). Light energy absorbed by photosystems I (PSI) and II (PSII) in the thylakoid membranes causes charge separation at the reaction-center chlorophylls, P700 in PSI and P680 in PSII, that drives the photosynthetic linear electron transport from H_2O on the donor side of PSII to the acceptor side of PSI via the interchain components, including plastoquinone, cytochrome b_6f complex, and plastocyanin (or cytochrome c_6). At the electron acceptor side of PSI, $NADP^+$ is reduced to NADPH with electrons from PSI via ferredoxin (Fd) and Fd-$NADP^+$ reductase. In these processes, the stromal proton is pumped into the luminal side of thylakoid membranes, resulting in a formation of proton gradient (ΔpH) across the thylakoid membranes, which provides the driving force for ATP production by ATP synthases in the thylakoid membranes. Generated ATP and NADPH are utilized for CO_2 reduction processes in the Calvin-Benson-Bassham (CBB) cycle. Although there is still a debate on the optimum ATP/NADPH requirement and on how it is modulated, it is widely accepted that photosynthetic electron transport and the CBB cycle is coupled as reflected in O_2 evolution and CO_2 consumption in the light.

Beside the CBB cycle, photosynthetic organisms harbor metabolic pathways that consumes NADPH (or reducing equivalents) generated by photosynthetic electron transport, which is so-called the alternative electron sink (AES). With a capacity comparable to the electron flow to the CBB cycle

✉ Ginga Shimakawa
gshimakawa@kwansei.ac.jp

[1] Department of Bioscience, School of Biological and Environmental Sciences, Kwansei Gakuin University, 1 Gakuen Uegahara, Sanda, Hyogo 669-1330, Japan

(Helman et al. 2003; Allahverdiyeva et al. 2013; Shimakawa et al. 2015), AES causes a discordance of the photosynthetic stoichiometry between O_2 evolution in PSII and CO_2 fixation in the CBB cycle. For example, in cyanobacteria and green algae, flavodiiron proteins (Flv) mediate O_2 photoreduction with reduced Fd as the electron donor at a comparable flux to the CBB cycle (Helman et al. 2003; Chaux et al. 2017; Sétif et al. 2020), which maintains the electron transport activity even without CO_2 fixation to dissipate excess light energy (Allahverdiyeva et al. 2013). Additionally, AES can modulate the production ratio of ATP (or ΔpH) to NADPH (or reducing equivalents) (Hasunuma et al. 2014; Burlacot et al. 2018). In the green alga *Chlamydomonas reinhardtii*, thylakoid lumen acidification is required also for the dehydration of HCO_3^- to CO_2 by the α-type carbonic anhydrase (CA) in the thylakoid lumen to provide CO_2 for Rubisco in the pyrenoid during the process of biophysical CO_2-concentrating mechanism (CCM; Moroney and Ynalvez 2007; Mukherjee et al. 2019; He et al. 2023), which is energetically supported by Flv-mediated O_2 photoreduction and cyclic electron flow around PSI (Burlacot et al. 2022). These facts imply that an AES is commonly required to convert HCO_3^- to CO_2 for photosynthesis in microalgae harboring the pyrenoid-based CCM.

Marine diatoms are responsible for up to a half of ocean primary production (Falkowski et al. 1998; Field et al. 1998). This large proportion is due in part to the high efficiency of CO_2 fixation driven by the operation of CCM. In spite of low dissolved CO_2 concentration (at most 10 μM under current atmosphere at 25°C) further hindered by high pH/salinity and 10^4 times lower gas diffusion efficiency, the size of HCO_3^- pool is significantly large (*ca.* 2 mM) in marine environments (Raven 1997). Therefore, marine diatoms have evolved the CCM to efficiently utilize external HCO_3^- for photosynthesis. In the pennate species *Phaeodactylum tricornutum*, several CCM components have already been characterized (Matsuda et al. 2017). Solute carrier 4 type Na^+-dependent HCO_3^- transporters on the plasma membrane actively take up HCO_3^- from seawater (Nakajima et al. 2013; Nawaly et al. 2022) most probably utilizing light energy. The θ-type CA, Ptθ-CA1, localized in the lumen of the pyrenoid-penetrating thylakoid membranes dehydrates HCO_3^- to CO_2 within the luminal proton, which is the dominant flux of CO_2 supply to Rubisco in this diatom (Kikutani et al. 2016; Shimakawa et al. 2023). To drive these mechanisms in the CCM, the additional ΔpH should be required in *P. tricornutum* and it is possibly supported by AES as it is also observed in *C. reinhardtii* (Burlacot et al. 2022) because AES can enhance the production ratio of ATP (or ΔpH) to NADPH (or reducing equivalents) (Hasunuma et al. 2014; Burlacot et al. 2018). However, we could observe little O_2-dependent AES in *P. tricornutum* (Shimakawa et al. 2017), which is consistent with the lack of Flv in diatoms.

Previously, we analyzed the redox state of P700 during the illumination with a short-saturation pulse to investigate the molecular mechanisms of AES in a variety of photosynthetic organisms (Shimakawa et al. 2019). In cyanobacteria, green algae, and basal land plants, P700 was kept oxidized during the short flash even if the cells were adapted to the darkness, which is owing to the O_2-dependent AES mediated by Flv (Shimakawa and Miyake 2018; Shimakawa et al. 2019). Meanwhile, the diatom *P. tricornutum* showed P700 oxidation even in the absence of O_2 (Shimakawa et al. 2019), implying that *P. tricornutum* develops the AES with an alternative electron acceptor other than O_2 (hereafter it is termed as "O_2-independent AES").

Theoretically, the O_2-independent AES can function in generating the additional ΔpH for the CO_2-evolving machinery in the CCM of diatoms if it has the capacity comparable to the CBB cycle. In this case, an O_2-independent AES should result the O_2 evolution larger than CO_2 consumption by molar ratio in diatom cells. Indeed, the stoichiometrically excess O_2 evolution has been observed in literatures mainly with $^{14}CO_2$ measurements (Buesa 1980; Williams and Robertson 1991; Halsey et al. 2013). The so-called "photosynthetic quotient" defined as the ratio of O_2 evolution to CO_2 fixation has been evaluated in a variety of microalgae, ranging approximately 1.0 – 2.0 dependent on species and increasing ~ 7.0 in a specific growth condition such as nitrogen deprivation (Halsey and Jones 2015; Rehder et al. 2023; and also see the latest review Trentman et al. 2023). These experimental facts imply that marine diatoms have a large capacity of O_2-independent AES comparable to that of the CBB cycle. Although the extra O_2 evolution in algal photosynthesis has been well recognized as a physiological phenomenon, the molecular mechanism is still unclear. In the present study, we simultaneously analyzed O_2 and dissolved inorganic carbon (DIC) during photosynthesis of *P. tricornutum* at different DIC concentrations to extend the knowledges on the physiological functions and molecular mechanism of the O_2-independent AES in marine diatoms.

Results and discussion

To evaluate the in vivo capacity of O_2-independent AES, we simultaneously measured net O_2 evolution and DIC consumption. The *P. tricornutum* cells were cultured under 1% CO_2 (high CO_2, HC), where most of CCM components are suppressed (Ohno et al. 2011; Nakajima et al. 2013) except for Ptθ-CA1 and the CO_2-evolving machinery in the pyrenoid-penetrating thylakoid membranes (Shimakawa et al. 2023), and air-level CO_2 (low CO_2, LC). At the logarithmic growth phase, the cells were harvested and resuspended in a DIC-free artificial seawater. Subsequently, photosynthetic O_2 evolution was measured via an O_2 electrode. In the reaction

chamber, the diatom cells were illuminated with a white actinic light under N_2 gas bubbled to consume DIC from the cell mixture. During the measurement, 5 µL of aliquots of the cell suspension was taken from the O_2 electrode chamber and injected into a GC-FID at each time point to determine the concentration of total DIC ([DIC]) in the culture (black circles in Fig. 1A and B). With the decrease in [DIC], the increase of the O_2 concentration ([O_2] as indicated by blue lines in Fig. 1A and B) was slowed down to reach a CO_2 compensation point (Fig. 1A). In LC-grown cells, total DIC was once almost completely removed from the cell mixture to allow the cells to reach the CO_2 compensation point where no O_2 evolution was detected. Thereafter, $NaHCO_3$ was added to the cell mixture at 150 µM of the final concentration (at the time zero in Fig. 1B), which stimulated photosynthetic CO_2 assimilation that finally reached a CO_2 compensation point again due to a deprivation of DIC (in approximately 10 min, Fig. 1B). Net O_2 evolution rate was calculated from the trace of [O_2] at each time point where [DIC] was determined, indicating that the LC-grown cells showed the higher photosynthetic affinity with DIC than the HC-grown cells (Fig. 1C) due to the expression of CCM components as already reported in literature (e.g., Ohno et al. 2012). There is a dip of net O_2 evolution rate around 150 µM [DIC] in the LC-grown cells (Fig. 1C), because the photosynthesis was not fully activated at that time just after the DIC addition (Fig. 1B). Here, we note that the HC- and LC-grown cells mainly showed a CO_2-limited and -saturated photosynthesis in the range of [DIC] below 150 µM, respectively (Fig. 1C).

In this study, we found that the proportional increase in [O_2] always exceeded the decrease in [DIC]. We denoted the difference between [O_2] increase versus [DIC] consumption as "$\Delta[O_2] - \Delta[DIC]$" (Fig. 1A and B, red triangles). In both HC- and LC-grown cells, the ratio of net O_2 evolution to net amount of DIC consumption was about 1.5. More interestingly, the increase in $\Delta[O_2] - \Delta[DIC]$ showed a proportional relationship to the increase in [O_2] within the [DIC] range < 150 µM in both HC- and LC-grown cells (Fig. 1A and B, red triangles versus blue lines), suggesting that *P. tricornutum* showed the extra O_2 evolution coupled with CO_2 fixation in the CBB cycle in both CO_2-limited and -saturated photosynthesis. In principle, our measurement analyzed the same phenomenon identified by previous studies (Buesa 1980; Williams and Robertson 1991; Halsey et al. 2013) in the different way.

An internal storage of DIC (or organic compounds) might be one explanation for the extra O_2 evolution observed in *P. tricornutum* during photosynthesis because it can drive the CBB cycle and the related electron transport giving O_2 evolution in the absence of DIC added. To test this possibility, we estimated the pool size of the hypothetical carbon storage by four-times repeating the same experiment of Fig. 1B in LC-grown cells. During four rounds, the *P. tricornutum* cells repeatedly showed the O_2 evolution 1.5 times larger than the added DIC at a molar ratio, resulting in the total 900 µM O_2 (Fig. 2). This corresponds to 300 µM of CO_2 storage if we assume a tight coupling of photosynthetic light and dark reactions. Considering that the reaction mixture contained the diatom cells at 10 µg chlorophyll *a* mL^{-1}, the DIC pool size was estimated to be more than 30 µmol mg^{-1} chlorophyll *a*, which was within the range of the pool size of prefixed malate in a crassulacean acid metabolism (CAM) plant (*ca.* 150 µmol mg^{-1} total chlorophyll; Keeley and Busch 1984). Overall, it is possible that the extra O_2 evolution in *P. tricornutum* ascribed to a biochemical DIC storage if the diatom develops an extremely huge carbon pool like CAM plants.

As another possibility, AES that does not consume O_2 leads to the larger O_2 evolution than DIC consumption in *P. tricornutum*. In this study, we sought to further investigate the molecular mechanism of the O_2-independent AES by measuring the ratio of O_2 evolution to DIC consumption ($\Delta[O_2]/\Delta[DIC]$, nearly corresponding to photosynthetic quotient) in a variety of physiological conditions. In literature so far, several metabolic pathways have been proposed as the electron sink, including nitrogen assimilation and the biosynthesis of lipids, amino acids, and volatile organic compounds such as dimethyl sulfide (Halsey and Jones 2015). Further, Halsey and co-workers proposed that glyceraldehyde 3-phosphate (GAP) in the CBB cycle is metabolized in the oxidative pentose phosphate (OPP) pathway to recover NADPH and CO_2, which can result in the extra net O_2 evolution if the regenerated NADPH is not used as the electron donor for O_2-reducing metabolisms. Among these candidates, nitrogen assimilatory reactions are one plausible candidate for the molecular mechanism of the large O_2-independent AES (Weger and Turpin 1989; Laws 1991; Lomas et al. 2000), including nitrate/nitrite reductions and glutamate synthesis, catalyzed by nitrate (and nitrite) reductases and glutamine oxoglutarate aminotransferase (GOGAT) respectively, both of which require reduced Fd (or its reducing equivalents) as the electron donor. Here, we measured $\Delta[O_2]/\Delta[DIC]$ in the *P. tricornutum* cells grown with NH_4Cl as the nitrogen source, instead of $NaNO_3$, and additionally in the presence of L-methionine sulfoximine that is an inhibitor to glutamine synthetase (Zehr and Falkowski 1988). Finally, we could not obtain any evidence that nitrogen assimilation functions as an electron sink coupling with photosynthetic electron transport in *P. tricornutum* (Fig. 3). The $\Delta[O_2]/\Delta[DIC]$ ratio increased to about 2.5 in the cells cultured under nitrogen starvation for 2 days (Fig. 3), which was consistent with literature (Halsey and Jones 2015). In the nitrogen-starved cells, the maximum net O_2 evolution rate decreased to approximately 68.3 ± 1.0 µmol (mg chlorophyll *a*)$^{-1}$ h^{-1} ($n = 3$, biological replicates),

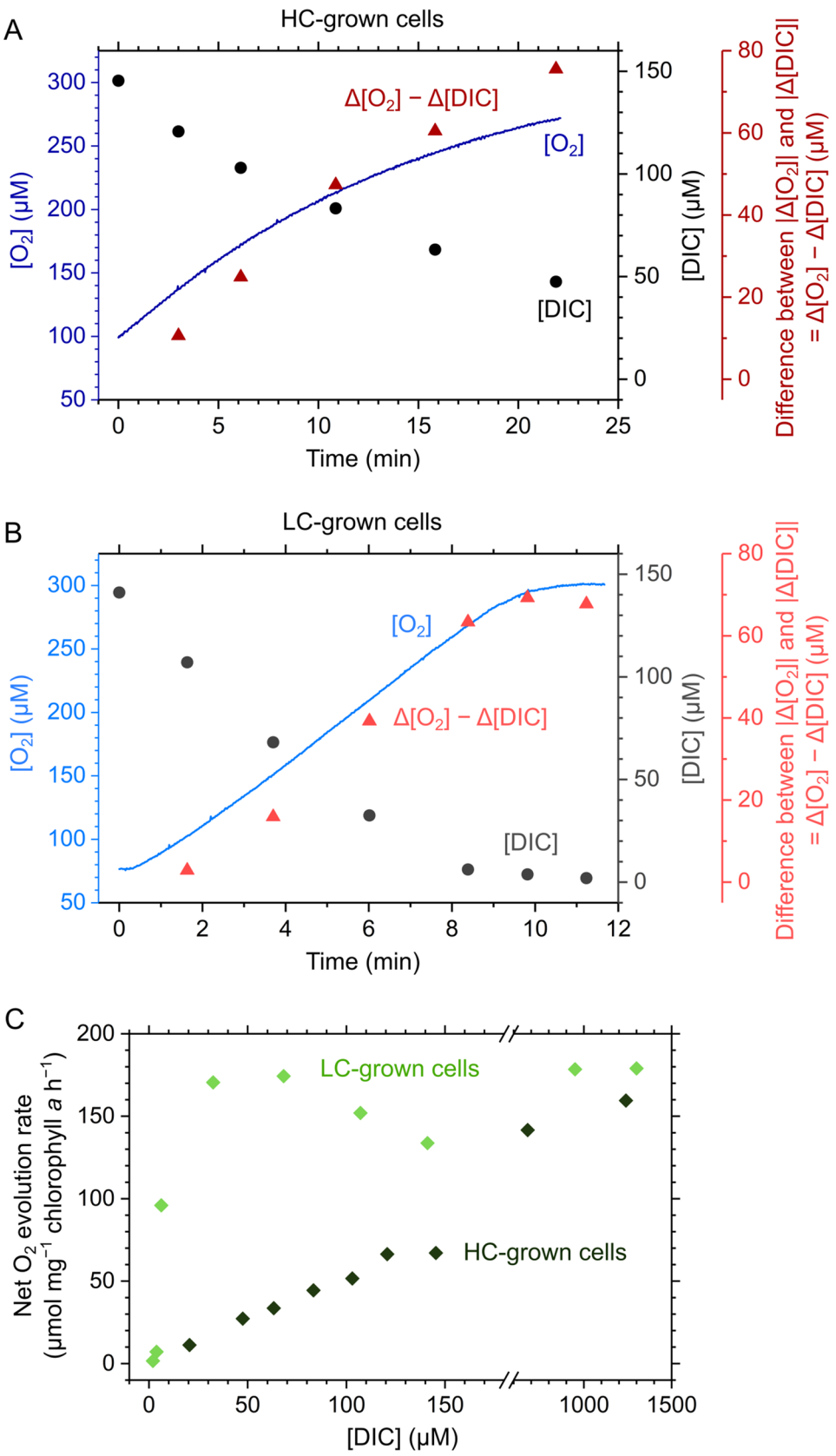

Fig. 1 O_2 evolution and dissolved inorganic carbon (DIC) consumption in the photosynthesis of *Phaeodactylum tricornutum*. **A**, **B** The increase in $[O_2]$ (blue lines) and the decrease in [DIC] (black circles) by photosynthesis of the cells grown under 1% (HC; **A**) and air-level CO_2 (LC; **B**). The difference between O_2 evolution and DIC consumption was calculated as "$\Delta[O_2] - \Delta[DIC]$" as shown in red triangles. For the measurements in LC-grown cells, 150 μM of $NaHCO_3$ was added at the time zero after the cells reached a CO_2-compensation point (see the text for details). **C** Dependency of net photosynthetic O_2 evolution rate on [DIC] calculated from Fig. 1A and B. Representative data of independent experiments (HC: $n = 3$; LC: $n = 5$) are shown, and the data of each two more replicates are shown in Supplementary Fig. S1

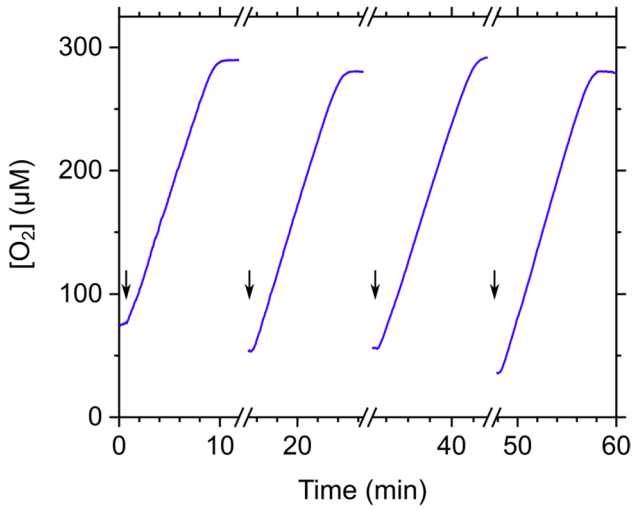

Fig. 2 Intermittent induction of photosynthesis by the additions of dissolved inorganic carbon (DIC) in *Phaeodactylum tricornutum* grown under air-level CO_2. 150 μM of $NaHCO_3$ was added to the reaction mixture at each time as indicated by arrows. Before the DIC additions, the mixture was bubbled with N_2 gas to avoid the $[O_2]$ signal to go beyond a detection limit of the electrode. Representative data of three independent experiments are shown

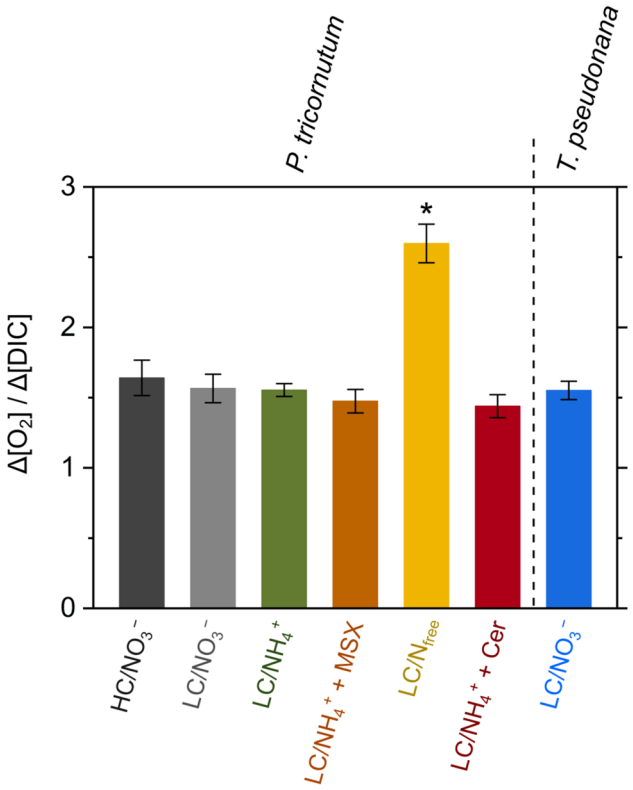

Fig. 3 Ratio of net O_2 evolution to the consumption of dissolved inorganic carbon (DIC), termed as $\Delta[O_2]/\Delta[DIC]$, in *Phaeodactylum tricornutum* and *Thalassiosira pseudonana*. The diatom cells were grown under 1% (HC) and air-level CO_2 (LC) in different nitrogen conditions: NO_3^-, 0.88 mM nitrate; NH_4^+, 0.88 mM ammonium. The nitrogen-starved cells (N_{free}) were prepared from the NH_4^+-cells after 2 days culture without nitrogen source. For the measurements, 150 μM of $NaHCO_3$ was added to the cells at the CO_2 compensation point as in Fig. 1A and B. Methionine sulfoximine (MSX) and cerulenin (Cer) were added at 10 mM and 100 μM of the final concentrations, respectively. Data are shown as the mean with the standard deviation of 3–5 independent experiments. Asterisk shows the significant difference from the value of LC/ NO_3^- by Student's *t* test ($p < 0.05$)

which corresponds to about 40% of that in non-starved cells. These facts suggested that the CBB cycle was depressed under nitrogen starvation approximately 3 times severely than the metabolism(s) related to the O_2-independent AES. We further tested the possibility that a metabolism related to lipid biosynthesis functions as the electron sink in the presence of cerulenin, an inhibitor to ketoacyl-ACP synthase. But the result was again negative (Fig. 3). Finally, we observed the same ratio of $\Delta[O_2]/\Delta[DIC]$ in the centric diatom *Thalassiosira pseudonana* (Fig. 3), which suggested that the O_2-independent AES commonly functions in marine diatoms at the similar flux.

Conclusion

In this study, we quantitatively evaluated the extra O_2 evolution in marine diatoms by the simultaneous measurements of $[O_2]$ and [DIC] in the cell suspensions during photosynthesis. Our measurements revisited the physiological phenomenon showing larger O_2 evolution than DIC consumption, which was previously observed in a variety of microalgae, including cyanobacteria, green algae, and secondary algae (Buesa 1980; Williams and Robertson 1991; Halsey et al. 2013). This phenomenon is, in principle, derived from metabolism(s) utilizing reductants generated in the photosynthetic electron transport system without consuming O_2. Most strikingly, the electron flux giving the extra O_2 evolution was estimated to be a half of that for CO_2 fixation in the CBB cycle in *P. tricornutum* and *T. pseudonana* (Figs. 1, 2, 3). The large AES capacity would sufficiently support the lumen acidification for the dehydration of HCO_3^- in the pyrenoid-penetrating thylakoid membranes in marine diatoms. Previously, we found that *P. tricornutum* can keep P700 oxidized in response to a saturation flash even in the absence of O_2 (Shimakawa et al. 2019), which agrees with the O_2-independent AES observed in this study.

Here, we extended the understandings for the molecular mechanism of the O_2-independent AES in marine diatoms. First, net O_2 evolution rate clearly shows a proportional relationship with relative electron transport rate at PSII through the intercept at almost zero at various light intensities in a CO_2-saturated condition (Shimakawa et al. 2017). Second, net O_2 evolution was not observed at the CO_2-compensation point (Fig. 1). Finally, the increase of $\Delta[O_2] - \Delta[DIC]$ was

proportional to the decrease of [DIC] (Fig. 1). These facts suggest that the electron flux to the O_2-independent AES is tightly associated with the CBB cycle. Based on this point, it is plausible that the OPP pathway regenerates NADPH and CO_2 coupled with the CBB cycle via the intermediate GAP (Halsey et al. 2011, 2013). Since the OPP pathway in *P. tricornutum* is restricted in the cytosol (Gruber et al. 2009), the proposed co-operation of the CBB cycle with the OPP pathway functions as a redox shuttle system between chloroplasts and the cytosol (Behrenfeld et al. 2004; Bailleul et al. 2015), which can be supported by triose-phosphate/phosphate translocators (Moog et al. 2015). We note that this system is responsible for the extra O_2 evolution only when the regenerated NADPH in the OPP pathway does not function as the electron donor for O_2-consuming metabolisms such as mitochondrial respiration. Importantly, the final electron acceptor(s) in the cytosol are still unclear. The present results suggest that nitrogen assimilation, including the processes catalyzed by nitrate/nitrite reductase and GOGAT, was not likely to contribute to the O_2-independent AES. Meanwhile, we could not exclude lipid biosynthesis as the candidate of O_2-independent AES because not all electron-consuming processes seem to be inhibited in the presence of cerulenin in marine diatoms (Suhaimi et al. 2022). In the chloroplasts of *P. tricornutum*, an ornithine cycle might function as the AES (Smith et al. 2016). Although the molecular mechanism of the O_2-independent AES remains to be studied by genetic-engineering techniques in the future, ultimately fully unknown proteins may be responsible for the AES observed in this study.

Materials and methods

Cultures

The marine pennate diatom *P. tricornutum* (UTEX642) and the centric diatom *T. pseudonana* (Hustedt) Hasle et Heimdal (CCMP 1335) were axenically and photoautotrophically cultured in the artificial seawater medium with the addition of 0.31% half-strength Guillard's 'F' solution (Guillard and Ryther 1962; Guillard 1975) under continuous light (20 °C, 40 µmol photons m^{-2} s^{-1}, fluorescent lamp) in flasks gently bubbled with ambient air or 1% (v/v) CO_2 supplemented air. For the growth in different nitrogen conditions, the pre-cultured cells in the NO_3^- medium were centrifugally washed twice in fresh NO_3^- or NH_4^+ media, and then inoculated to each medium, respectively. After 3 – 4 days culture, the cells at the logarithmic growth phase were used for experiments. For the preparation of nitrogen-starved cells, the 3-days culture in the NH_4^+ medium (early logarithmic growth phase) was inoculated to the nitrogen-free medium, and then cultured for 2 days.

Photosynthesis measurement

The centrifugally harvested diatom cells were resuspended in a DIC-free F/2 artificial sea water (pH 8.15) freshly prepared. The reaction medium contained the cells at 5 – 20 µg chlorophyll *a* mL^{-1}, and the exact chlorophyll concentration was determined in 100% (v/v) methanol after the photosynthesis measurements (Jeffrey and Haxo 1968). Net O_2 evolution was measured by an O_2 electrode (Hansatech, King's Lynn, U.K.), total DIC concentration was simultaneously determined by GC-FID (GC-8A, Shimadzu, Kyoto, Japan; Shimakawa et al. 2023). The freshly prepared artificial seawater contained 10 mM Tris–HCl, and the pH was not affected by the addition of 150 µM $NaHCO_3$.

Supplementary Information The online version contains supplementary material available at https://doi.org/10.1007/s11120-023-01073-3.

Acknowledgements We would like to thank Dr. Matthew B. Brown (Kwansei Gakuin University) for many helpful advices and for kindly proofreading our English writing.

Author contributions GS designed the research plans, performed the experiments, analyzed the data, and wrote the manuscript with the assistance from YM.

Funding This work was supported by Japan Society for the Promotion of Science (JSPS) KAKENHI (19H01153 to G.S. and Y.M.) and by JST CREST "Cell dynamics" (JPMJCR20E1 to Y.M.).

Data availability The data of physiological analyses in this manuscript are available from the corresponding author upon request.

Declarations

Conflict of interest The authors have no conflict of interest to declare.

References

Allahverdiyeva Y, Mustila H, Ermakova M, Bersanini L, Richaud P, Ajlani G et al (2013) Flavodiiron proteins Flv1 and Flv3 enable cyanobacterial growth and photosynthesis under fluctuating light. Proc Natl Acad Sci USA 110:4111–4116

Bailleul B, Berne N, Murik O, Petroutsos D, Prihoda J, Tanaka A et al (2015) Energetic coupling between plastids and mitochondria drives CO_2 assimilation in diatoms. Nature 524:366–369

Behrenfeld MJ, Prasil O, Babin M, Bruyant F (2004) In search of a physiological basis for covariations in light-limited and light-saturated photosynthesis. J Phycol 40:4–25

Bishop N (1971) Photosynthesis: the electron transport system of green plants. Annu Rev Biochem 40:197–226

Buesa R (1980) Photosynthetic quotient of marine plants. Photosynthetica 14:337–342

Burlacot A, Sawyer A, Cuiné S, Auroy-Tarrago P, Blangy S, Happe T, Peltier G (2018) Flavodiiron-mediated O_2 photoreduction links H_2 production with CO_2 fixation during the anaerobic induction of photosynthesis. Plant Physiol 177:1639–1649

Burlacot A, Dao O, Auroy P, Cuiné S, Li-Beisson Y, Peltier G (2022) Alternative photosynthesis pathways drive the algal CO_2-concentrating mechanism. Nature 605:366–371

Chaux F, Burlacot A, Mekhalfi M, Auroy P, Blangy S, Richaud P et al (2017) Flavodiiron proteins promote fast and transient O_2 photoreduction in Chlamydomonas. Plant Physiol 174:1825–1836

Falkowski PG, Barber RT, Smetacek V (1998) Biogeochemical controls and feedbacks on ocean primary production. Science 281:200–206

Farquhar GD, von Caemmerer S, Berry JA (1980) A biochemical model of photosynthetic CO_2 assimilation in leaves of C_3 species. Planta 149:78–90

Field CB, Behrenfeld MJ, Randerson JT, Falkowski P (1998) Primary production of the biosphere: Integrating terrestrial and oceanic components. Science 281:237–240

Gruber A, Weber T, Bártulos CR, Vugrinec S, Kroth PG (2009) Intracellular distribution of the reductive and oxidative pentose phosphate pathways in two diatoms. J Basic Microbiol 49:58–72

Guillard RRL (1975) Culture of phytoplankton for feeding marine invertebrates. In: Smith WL, Chanley MH (eds) Culture of marine invertebrate animals. Springer, Boston, pp 29–60

Guillard RRL, Ryther JH (1962) Studies of marine planktonic diatoms: I. *Cyclotella nana* hustedt, and *Detonula confervacea* (cleve) gran. Can J Microbiol 8:229–239

Halsey KH, Jones BM (2015) Phytoplankton strategies for photosynthetic energy allocation. Annu Rev Mar Sci 7:265–297

Halsey KH, Milligan AJ, Behrenfeld MJ (2011) Linking time-dependent carbon-fixation efficiencies in *Dunaliella tertiolecta* (Chlorophyceae) to underlying metabolic pathways. J Phycol 47:66–76

Halsey KH, O'Malley RT, Graff JR, Milligan AJ, Behrenfeld MJ (2013) A common partitioning strategy for photosynthetic products in evolutionarily distinct phytoplankton species. New Phytol 198:1030–1038

Hasunuma T, Matsuda M, Senga Y, Aikawa S, Toyoshima M, Shimakawa G, Miyake C, Kondo A (2014) Overexpression of flv3 improves photosynthesis in the cyanobacterium *Synechocystis* sp. PCC6803 by enhancement of alternative electron flow. Biotechnol Biofuels 7:493

He S, Crans VL, Jonikas MC (2023) The pyrenoid: the eukaryotic CO_2-concentrating organelle. Plant Cell 35:3236−3259

Helman Y, Tchernov D, Reinhold L, Shibata M, Ogawa T, Schwarz R et al (2003) Genes encoding A-type flavoproteins are essential for photoreduction of O_2 in cyanobacteria. Curr Biol 13:230–235

Jeffrey S, Haxo F (1968) Photosynthetic pigments of symbiotic dinoflagellates (zooxanthellae) from corals and clams. Biol Bull 135:149–165

Keeley JE, Busch G (1984) Carbon assimilation characteristics of the aquatic CAM plant. Isoetes Howellii Plant Physiol 76:525–530

Kikutani S, Nakajima K, Nagasato C, Tsuji Y, Miyatake A, Matsuda Y (2016) Thylakoid luminal θ-carbonic anhydrase critical for growth and photosynthesis in the marine diatom *Phaeodactylum tricornutum*. Proc Natl Acad Sci USA 113:9828–9833

Laws EA (1991) Photosynthetic quotients, new production and net community production in the open ocean. Deep Sea Res Part A 38:143–167

Lomas MW, Rumbley CJ, Glibert PM (2000) Ammonium release by nitrogen sufficient diatoms in response to rapid increases in irradiance. J Plankton Res 22:2351–2366

Matsuda, Y., Hopkinson, B.M., Nakajima, K., Dupont, C.L. and Tsuji, Y. (2017) Mechanisms of carbon dioxide acquisition and CO_2 sensing in marine diatoms: a gateway to carbon metabolism. *Philos Trans R Soc Lond B Biol Sci* 372.

Moog D, Rensing SA, Archibald JM, Maier UG, Ullrich KK (2015) Localization and evolution of putative triose phosphate translocators in the diatom *Phaeodactylum tricornutum*. Genome Biol Evol 7:2955–2969

Moroney JV, Ynalvez RA (2007) Proposed carbon dioxide concentrating mechanism in *Chlamydomonas reinhardtii*. Eukaryot Cell 6:1251–1259

Mukherjee A, Lau CS, Walker CE, Rai AK, Prejean CI, Yates G et al (2019) Thylakoid localized bestrophin-like proteins are essential for the CO_2 concentrating mechanism of *Chlamydomonas reinhardtii*. Proc Natl Acad Sci USA 116:16915–16920

Nakajima K, Tanaka A, Matsuda Y (2013) SLC4 family transporters in a marine diatom directly pump bicarbonate from seawater. Proc Natl Acad Sci 110:1767–1772

Nawaly H, Matsui H, Tsuji Y, Iwayama K, Ohashi H, Nakajima K et al (2022) Multiple plasma membrane SLC4s contribute to external HCO_3^- acquisition during CO_2 starvation in the marine diatom *Phaeodactylum tricornutum*. J Exp Bot 74:296–307

Ohno N, Inoue T, Yamashiki R, Nakajima K, Kitahara Y, Ishibashi M et al (2012) CO_2-cAMP-responsive *cis*-elements targeted by a transcription factor with CREB/ATF-like basic zipper domain in the marine diatom *Phaeodactylum tricornutum*. Plant Physiol 158:499–513

Raven JA (1997) CO_2-concentrating mechanisms: a direct role for thylakoid lumen acidification? Plant Cell Environ 20:147–154

Rehder L, Rost B, Rokitta SD (2023) Abrupt and acclimation responses to changing temperature elicit divergent physiological effects in the diatom *Phaeodactylum tricornutum*. New Phytol 239:1005–1013

Sétif P, Shimakawa G, Krieger-Liszkay A, Miyake C (2020) Identification of the electron donor to flavodiiron proteins in *Synechocystis* sp. PCC 6803 by in vivo spectroscopy. Biochim Biophys Acta Bioenerg 1861:148256

Shimakawa G, Miyake C (2018) Oxidation of P700 ensures robust photosynthesis. Front Plant Sci 9:1617

Shimakawa G, Shaku K, Nishi A, Hayashi R, Yamamoto H, Sakamoto K et al (2015) FLAVODIIRON2 and FLAVODIIRON4 proteins mediate an oxygen-dependent alternative electron flow in *Synechocystis* sp. PCC 6803 under CO_2-limited conditions. Plant Physiol 167:472–480

Shimakawa G, Matsuda Y, Nakajima K, Tamoi M, Shigeoka S, Miyake C (2017) Diverse strategies of O_2 usage for preventing photo-oxidative damage under CO_2 limitation during algal photosynthesis. Sci Rep 7:41022

Shimakawa G, Murakami A, Niwa K, Matsuda Y, Wada A, Miyake C (2019) Comparative analysis of strategies to prepare electron sinks in aquatic photoautotrophs. Photosynth Res 139:401–411

Shimakawa G, Okuyama A, Harada H, Nakagaito S, Toyoshima Y, Nagata K et al (2023) Pyrenoid-core CO_2-evolving machinery is essential for diatom photosynthesis in elevated CO_2. Plant Physiol 193:2298−2305

Smith SR, Gillard JTF, Kustka AB, McCrow JP, Badger JH, Zheng H et al (2016) Transcriptional orchestration of the global cellular response of a model pennate diatom to diel light cycling under iron limitation. PLoS Genet 12:e1006490

Suhaimi N, Maeda Y, Yoshino T, Tanaka T (2022) Effects of fatty acid synthase-inhibitors on polyunsaturated fatty acid production in marine diatom *Fistulifera solaris* JPCC DA0580. J Biosci Bioeng 133:340–346

Trentman MT, Hall RO Jr, Valett HM (2023) Exploring the mismatch between the theory and application of photosynthetic quotients in aquatic ecosystems. Limnol Oceanogr Lett 8:565–579

Weger HG, Turpin DH (1989) Mitochondrial respiration can support NO_3^- and NO_2^- reduction during photosynthesis: Interactions between photosynthesis, respiration, and N assimilation in the N-limited green alga *Selenastrum minutum*. Plant Physiol 89:409–415

Williams PJI, Robertson JE (1991) Overall planktonic oxygen and carbon dioxide metabolisms: the problem of reconciling observations

and calculations of photosynthetic quotients. J Plankton Res 13:153–169
Zehr JP, Falkowski PG (1988) Pathway of ammonium assimilation in a marine diatom determined with the radiotracer ^{13}N. J Phycol 24:588–591